



# Procurement and Characterization of Biodegradable Films made from Blends of Eucalyptus, Pine and Cocoa Bean Shell Nanocelluloses

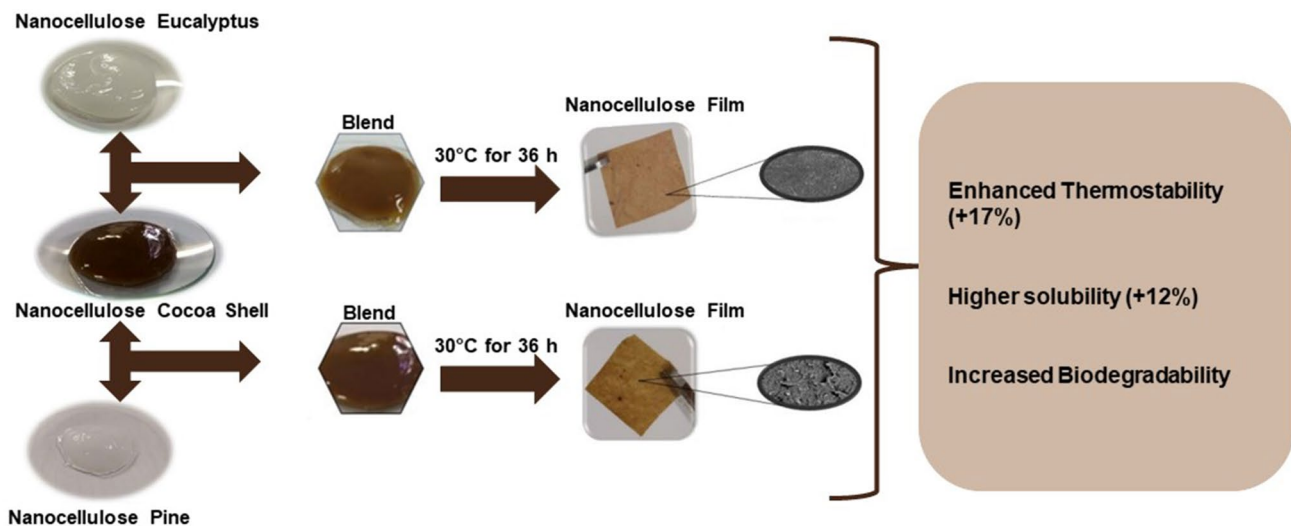
Lucas Oliveira Souza<sup>1</sup> · Ingrid Alves Santos<sup>1</sup> · Iasnaia Maria de Carvalho Tavares<sup>1</sup> · Igor Carvalho Fontes Sampaio<sup>2</sup> · Matheus Cordazzo Dias<sup>3</sup> · Gustavo Henrique Denzin Tonoli<sup>3</sup> · Elisângela Elena Nunes de Carvalho<sup>4</sup> · Eduardo Valério de Barros Vilas Boas<sup>4</sup> · Muhammad Irfan<sup>5</sup> · Muhammad Bilal<sup>6</sup> · Julieta Rangel de Oliveira<sup>7</sup> · Marcelo Franco<sup>7</sup>

Received: 9 December 2021 / Accepted: 27 March 2022 / Published online: 16 April 2022  
© The Author(s), under exclusive licence to Springer Nature B.V. 2022

## Abstract

The objective of this work was to investigate the effect of the addition of a nanocellulose gel from cocoa bean husk (NAC) on nanocellulose gels of *Eucalyptus* sp. and *Pinus* sp. The nanogels were obtained by mechanical defibrillation and the films by casting with different concentrations of NAC (0%, 20% and 35%). These were evaluated for morphology, thermogravimetric properties, barrier properties and soil biodegradability. NAC fibres presented the shortest lengths (30–80 µm), and their addition to the films reduced degradation at 350 °C by 17% but did not cause changes in water vapor permeability. NAC increased the solubility and biodegradability of the films, especially those of *Eucalyptus* sp. (35%). Therefore, the use of NAC proved to be a promising tool in the formulation of biodegradable packaging.

## Graphical Abstract



**Keywords** Nanofibrils · *Theobroma cacao* L. · Agro-industrial co-products · Nanomaterials · Lignocellulose

## Abbreviations

NAC Cocoa bean shell nanocellulosic gel  
WVP Water vapor permeability

CNF Nanofibrillated cellulose  
NEL Eucalyptus nanocellulosic gel  
PIN Pine nanocellulosic gel  
NEL20% Film with 20% NAC and 80% NEL  
NEL35% Film with 35% NAC and 65% NEL  
PIN20% Film with 20% NAC and 80% PIN

✉ Marcelo Franco  
mfranco@uesc.br

Extended author information available on the last page of the article

PIN35%	Film with 35% NAC and 65% PIN
OM	Optical microscopy
SEM	Scanning electron microscopy
TGA	Thermogravimetric analysis
AC	Contact angle

## Statement of Novelty

This work presents the technological potential of nanocellulosic gels produced through agro-industrial co-products. The nanocellulosic gel from cocoa bean shell was added at different concentrations to eucalyptus and pine gels to obtain biodegradable films. The addition of nanofibers from the cocoa bean shell promoted greater biodegradability, solubility and thermal stability to the films. These become, therefore, sustainable materials with potential use for making food packaging, coatings and coverings, in addition to enabling the reduction in the use of petroleum-derived polymers.

## Introduction

The demand for sustainable materials has increased in recent years due to the growing need to replace synthetic, petroleum-derived polymers with natural ones, which would reduce the negative impact on the environment [1]. In this context, materials produced from natural polymers have gained great interest in the scientific community for their biodegradability [2].

The most abundant natural polymer is cellulose, a polysaccharide that has been the subject of several research studies and has shown potential applications in many areas. Examples of industrial sectors that make use of this compound are the food industry for packaging development [3], the biomedical industry for the development of dressings and drug carriers [4, 5] and the cosmetic industry for the production of facial masks [6]. The textile and paper industries are also making use of cellulose for the development of fabrics with improved properties [7] and the production of paper carrying bioactive compounds [8, 9], respectively.

Through physical, chemical or biological processes, cellulose can become a precursor of nanocellulose [10]. Mechanical defibrillation, for example, is a physical process that exposes surfaces previously located inside the fibres of the cellulosic material, which gives rise to cellulose on a reduced scale [11]. This process increases the surface area of contact of the cellulosic material, promoting improved traction, optical, electrical and chemical characteristics, which culminate in a more resistant, biodegradable material with superior gas barrier properties and thermal stability [12, 13]. After the defibrillation process, a gel called nanofibrillated cellulose (CNF) is obtained [11]. For all these properties,

nanocellulose is emerging as a revolutionary product, with market capital estimated at \$297 million in 2020 and projected to reach \$783 million in 2025 [14].

The most explored resource for obtaining CNF is wood from *Eucalyptus* sp. and *Pinus* sp. [15]; however, due to their high cellulose content (40–50%) [16] and low economic value, agro-industrial residues have aroused great interest [17, 18]. Among the agro-industrial residues that have already been used for the extraction of CNF are orange peel [19], sugarcane bagasse [20] and corn cobs [21]. Thus, several studies have been carried out with the objective of using these residues in the production of materials with greater added value, such as cellulose biocomposites [22].

The cocoa bean husk is a widely studied agro-industrial residue, e.g. for the production of a fermented solid for use in an organic medium [23], in the production of enzyme extracts with high activity [24–29], which have already been applied in the coagulation of milk [30], in the pre-treatment of leaves for essential oil extraction [31], and even in the manufacture of films to obtain biodegradable packaging [32–34]. In this context, the antioxidant capacity of the cocoa bean shell [34–39] and its cellulose content [39] makes it a promising source of CNF, as recently demonstrated by Souza et al. [32] when producing gel and Hoyos et al. [33] and Lessa et al. [34], when producing films, using only the cocoa bean shells as a cellulosic source. Furthermore, it is believed that the use of different sources of CNF in the production of cellulolytic blends can benefit the production of biocomposites. This is due to the fact that the interaction between the different gels can result in materials with improved mechanical strength, thermal strength, gas barrier properties and biodegradability [40].

Given the above, the present work aimed to investigate the formation of films by mixing nanocellulose gels from the shells of cocoa beans (*Theobroma cacao* L.), *Eucalyptus* sp. and *Pinus* sp. To unravel the effects of interactions of nanomaterials, analyses of morphological (optical microscopy [OM] and scanning electron microscopy [SEM]), thermogravimetric and chemical (contact angle [CA], water vapor permeability [WVP], solubility [S] and biodegradability) properties were performed.

## Materials and Methods

### Cellulosic Material

Cocoa bean shell (*Theobroma cacao* L.), supplied by agroindustries located in the city of Ilhéus (Bahia, Brazil), and bleached kraft pulps of eucalyptus (*Eucalyptus* sp.) and kraft pine pulps (*Pinus* sp.), supplied by the company Klabin SA (Paraná, Brazil), were used as cellulosic material.

## Production of Nanofibril Gels

Bleached eucalyptus (*Eucalyptus* sp.) and pine (*Pinus* sp.) pulps were hydrated at 2.0% (w/v), while the cocoa bean shell was hydrated at 4.0% (w/v) for 48 h. Afterwards, the samples were homogenized separately in a homogenizer (Tecnal, Turratec 102 Model, BRASIL®) at 8000 rpm for 1 h. Then, the suspensions were defibrillated (30 passes) separately in a SuperMassColloide microfibrillator (Masuko Sangyo MKGA6-80, Kawaguchi, Japan) equipped with two disks (MKGA6-80) with a rotation speed of 1500 rpm. Thus, gels of eucalyptus nanofibrils (NEL), pine (PIN) and cocoa bean shell (NAC) were obtained and stored at 4 °C.

## Preparation of Biodegradable Films

Biodegradable films were obtained using the solvent evaporation technique proposed by Guimarães et al. [41]. Table 1 shows the quantities of gels used in the preparation of each film, and the total mass used to prepare the gels was 5 g. The gels were homogenized at 500 rpm (Tecnal, Turratec 102 Model, BRASIL®) for 10 min at a temperature of 28 °C. Acrylic plates 15 cm in diameter were used as moulds to obtain the films after heat treatment at 30 °C for 36 h. After preparation, the films were stored in polyethylene bags at room temperature ( $\pm 25$  °C).

## Characterization

### Optical Microscopy (OM)

Nanofibril gel solutions (0.75%) prepared with distilled water were stained with an ethanol-safranin solution (1.0%) and visualized on an Olympus BX41 microscope coupled to an LC Color PL A662 camera (Tokyo, Japan) for image acquisition. The dissociation of cellular elements was performed according to Miranda and Castelo [42], and the images obtained were analysed to determine the mean diameter of nanofibrils and their distribution using ImageJ 1.48 software (National Institutes of Health, US).

**Table 1** Formulations used for the preparation of eucalyptus (NEL) and pine (PIN) nanocellulosic films and with the addition of cocoa bean shell gel (NAC)

Samples	Concentration (% w/w)		
	NEL	PIN	NAC
NEL	100	0	0
NEL20%	80	0	20
NEL35%	65	0	35
PIN	0	100	0
PIN20%	0	80	20
PIN35%	0	65	35

## Scanning Electron Microscopy (SEM)

The film samples were visualized in a scanning electron microscope, model QUANTA 250 (FEI COMPANY, Oregon, US), operating at an accelerating voltage of 15 kV. The films, approximately 0.5 cm<sup>2</sup> in area, were fixed to the ‘STUB’ supports with double-sided adhesive tape and submitted to metallization in an SCD 050 gold evaporator. Electron micrographs were acquired at 500× magnification.

## Thermogravimetric Analysis (TGA)

Non-isothermal experiments were performed in a Q 500 thermogravimetric analyser, Q series (TA Instruments, New Castle, DE), using a thermogravimetric detector module coupled to a thermal analyser, using a heating rate of 10 °C. min<sup>-1</sup> under a dynamic atmosphere of Nitrogen with a flow rate of 20 mL.min<sup>-1</sup>. Thermogravimetric analysis (TGA) curves were used to determine mass losses (%) and temperature ranges (°C). The sample mass of each biodegradable film was about 10 mg, and the maximum temperature of the aluminium holder was 500 °C. TGA curves were obtained with TRIOS Software (TA Instruments, New Castle, DE), and graphs were constructed with OriginPro 8.5 software (OriginLab Corp, Northampton, Ma, USA).

## Contact Angle (CA)

Film samples were cut to dimensions of 3 cm×10 cm and deposited on glass slides, which were installed on the base of a goniometer (Kruss, DSA25, Hamburg, Germany). Then, a drop of distilled water (10 µL) was applied under the samples, and images were captured by a micro camera for further analysis with the Advanced software (Kruss, Hamburg, Germany) [43].

## Water Vapor Permeability (WVP)

The WVP rate of the films was determined according to the standards of the American Society Testing and Materials Standard—E96-00—ASTM. The films, measuring approximately 5.25 mm<sup>2</sup>, were placed under the lid of a 40-mL amber glass bottle filled 3/4 of its volume with silica previously dried for 24 h at 150 °C. Openings 13.8 mm in diameter were made in the lid. The amber glasses containing the films were placed in hermetic desiccators at 19 °C with 800 mL of water inside the desiccator. The experiment was conducted in a controlled environment at 23±0.5 °C, and the glass bottles were weighed every 24 h for a period of 10 days. A calibration curve was constructed considering the weight gained by the silica over the evaluation period. Then, the water vapor permeability rate (WVPR) was calculated according to Eq. (1), with the water vapor transmission rate

of the biodegradable film being determined from the slope of the weight change graph of the bottle vs. time. WVP was calculated using Eq. (2) [44, 45]. Five repetitions were performed for each treatment.

$$\text{WVPR (g m}^2\text{dia}^{-1}) = gt \times A \quad (1)$$

where:  $gt$  is the slope of the straight-line equation (linear regression) and  $A$  is the permeation area ( $m^2$ ).

$$\text{WVP (g.mm.kPa}^{-1}\text{.dia}^{-1}\text{.m}^{-2}) = (\text{WVPR} \cdot E) \cdot \Delta p^{-1}, \quad (2)$$

where:  $E$  is the sample thickness (mm) and  $\Delta p$  is the saturation pressure of the steam at the test temperature (2.33921 kPa).

### Solubility in Water (S)

Samples of biodegradable films measuring  $5 \text{ cm}^2$  in diameter were dried in a drying oven with forced air circulation (TE-319, Tecnal, Piracicaba, Brazil) at a temperature of  $105 \text{ }^\circ\text{C}$  for 4 h until they reached a constant weight (BioPrecisa®—Electronic Scale; FA—2104 N). After this procedure, the films were immersed in a container containing 30 mL of distilled water and incubated at  $23 \text{ }^\circ\text{C}$  and 50 rpm for 24 h. After incubation, the films were dried at  $105 \text{ }^\circ\text{C}$  for 4 h and weighed. Then, the resulting suspensions were filtered, and the non-solubilized materials were dried in an incubator with circulating air at  $105 \text{ }^\circ\text{C}$  for 24 h and then weighed. The solubility (S) was calculated according to Eq. (3) and expressed as a percentage.

$$S(\%) = \left( \frac{PI - PF}{PI} \right) \times 100, \quad (3)$$

where:  $PI$  is the initial mass of dry material and  $PF$  is the final mass of non-solubilized dry material.

### Biodegradability in Soil

The biodegradability test followed the procedure proposed by Costa et al. [46]. Films measuring approximately  $5 \text{ cm}^2$  were dried in an oven with forced-air circulation (TE-319, Tecnal, Piracicaba, Brazil) at  $105 \text{ }^\circ\text{C}$  for 4 h until they reached a constant weight (ACB LABOR®). After this procedure, the films were placed on the surface of a PVC plastic container containing a mixture of 500 g of clay and fertile soil. The samples were incubated at  $30 \text{ }^\circ\text{C}$  for 1008 h, and the biofilms were weighed at intervals of 168 h.

### Data Analysis

A completely randomized design (CRD) was employed, with the addition of three NAC factors (0%, 20% and 35%) to the NEL and PIN films (controls). For each treatment,

three repetitions were performed. Data were subjected to analysis of variance (ANOVA), mean and standard deviation. Means were compared by Tukey's test ( $p \leq 0.05$ ), using PAST 3.19 (PAleontological STATistical).

## Results and Discussion

### Optical Microscopy (OM)

The morphology of the shell fibres of cocoa, eucalyptus and pine beans after the mechanical defibrillation process was determined from the OM images. Individualized and uniform cocoa bean shell fibres can be seen (Fig. 1a). On the other hand, eucalyptus and pine fibres were structurally heterogeneous and susceptible to entanglement and agglomeration (Fig. 1b, c).

The nanofibers from the cocoa bean shell were the ones that presented a smaller proportional length, around  $30\text{--}80 \text{ }\mu\text{m}$  (Fig. 1d). Already, the eucalyptus and pine nanofibers, evaluated outside the agglomeration zone, presented lengths of approximately  $150\text{--}180 \text{ }\mu\text{m}$  and  $180\text{--}210 \text{ }\mu\text{m}$ , respectively. The greater length of the pine nanofibers justifies the greater formation of agglomerates, as these occur due to the strong hydrogen bonds formed between the  $\text{--OH}$  groups of the cellulose, which, consequently, induce greater formation of aggregated fibres [13].

The length values of cocoa bean shell nanofibers were lower than those found for soy shell nanofibers ( $50\text{--}170 \text{ }\mu\text{m}$ ) [47], pineapple residue ( $300\text{--}900 \text{ }\mu\text{m}$ ) [48] and rice straw ( $400\text{--}3400 \text{ }\mu\text{m}$ ) [49]. On the other hand, the length measurements of eucalyptus and pine nanofibers indicated proximity to the soy shell nanofibers and inferiority to the nanofibers of pineapple residue and rice straw.

Regarding the diameter, eucalyptus and pine nanofibers presented values between 4 and  $5 \text{ }\mu\text{m}$ , lower than those observed for pure cotton fibres ( $14\text{--}30 \text{ }\mu\text{m}$ ) [50] and *Helicteres isora* ( $10\text{--}20 \text{ }\mu\text{m}$ ) [51]. On the other hand, the length of nanofibers from the cocoa bean shell was concentrated between 5 and  $6 \text{ }\mu\text{m}$  (Fig. 1e), approaching those of nanofibers from soy shells ( $6\text{--}8 \text{ }\mu\text{m}$ ) and rice straw ( $5\text{--}9 \text{ }\mu\text{m}$ ) [49].

The differences between the length and diameter of the shells of cocoa, eucalyptus and pine beans occur as a function of the morphological characteristics of the cellulosic material and, mainly, the amount of cellobiose monomers present in the formation of cellulose chains [52]. This is because the parallel stacking of multiple cellulosic chains determines the structural dimensions (length and diameter) of the microfibrils, which aggregate in an organized manner in the formation of cellulose fibres [52].



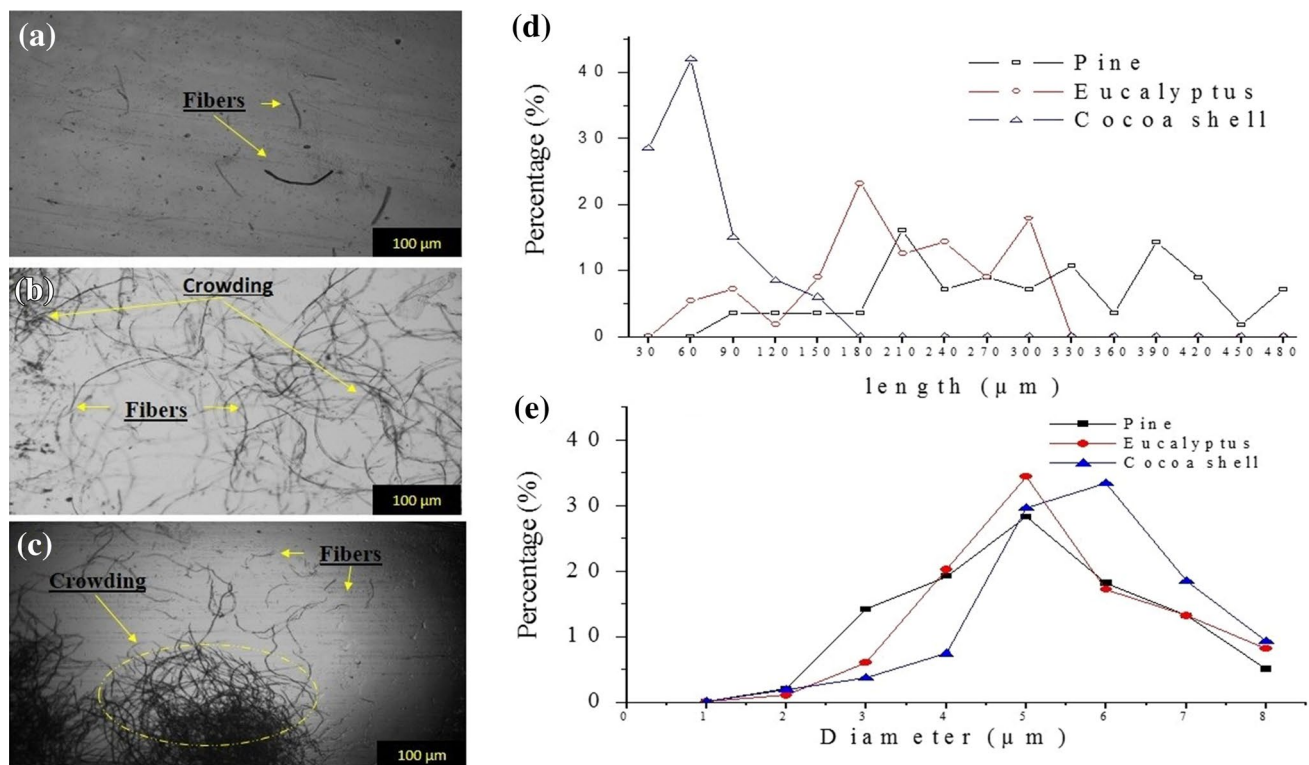


**Fig. 1** Optical microscopy of fiber from: **a** cocoa bean shell; **b** eucalyptus; **c** pine; **d** length distribution of cocoa, eucalyptus and pine shell fibers and **e** width distribution of cocoa, eucalyptus and pine shell fibers

## Scanning Electron Microscopy (SEM)

The NEL films observed by SEM (Fig. 2a-c) presented a structure with roughness and small surface deformations, unlike the PIN films (Fig. 2d-f), which presented a more heterogeneous surface and more fractures. The difference in surface layer heterogeneity of the NEL and PIN films is related to the structural dimensions of the nanofibers, with pine nanofibers being larger and more susceptible to stacking than those of eucalyptus, as demonstrated in the OM. According to Dias et al. [17], the high aggregation of fibres occurs due to their strong tendency to form hydrogen bonds, causing the fibres to concentrate in certain regions. Azeredo et al. [53] also reported that fibre aggregations are formed due to intra- and intermolecular hydrogen interactions between various hydroxyl groups of nanocellulose. Thus, it is possible that PIN films are more likely to form hydrogen bond interactions, culminating in the formation of the observed aggregates.

As shown in the SEM micrographs, the films containing NAC (Fig. 2b,c,d,e,f) showed a more heterogeneous surface with the presence of high apertures, unlike the NEL (Fig. 2a) and PIN (Fig. 2d) films. It is believed that this difference consists in the fact that films containing NAC have non-cellulosic components such as tracheids, hemicellulose and

lignin, which interact with NEL and PIN fibres, intensifying the formation of aggregates in the films and making their surface irregular [54]. In this sense, the addition of higher levels of NAC (35%) to the films promoted the presence of greater irregularities on the film surface, probably due to the presence of non-cellulosic components that were found in greater amounts in the mixture [54].

Similar results were also reported in biocomposites containing nanofibrillated cellulose from beet pulp and liquorice residue, with greater heterogeneity when pores were present in the films with higher levels of nanofibrillated cellulose in the respective substrates [55, 56]. The irregularities present in these samples were justified by the possible existence of hydroxyl groups on the surfaces of the fibres, which interact with each other and cause selective agglomeration during the drying process. Therefore, the films produced in this work were similar to those made from other vegetable cellulosic sources, which demonstrates the functionality of cocoa shell as an input source for the production of nanocellulose.

## Thermogravimetric Analysis (TGA)

The thermal decomposition mechanism of the NEL (Fig. 3a) and PIN (Fig. 3b) films with and without the addition of

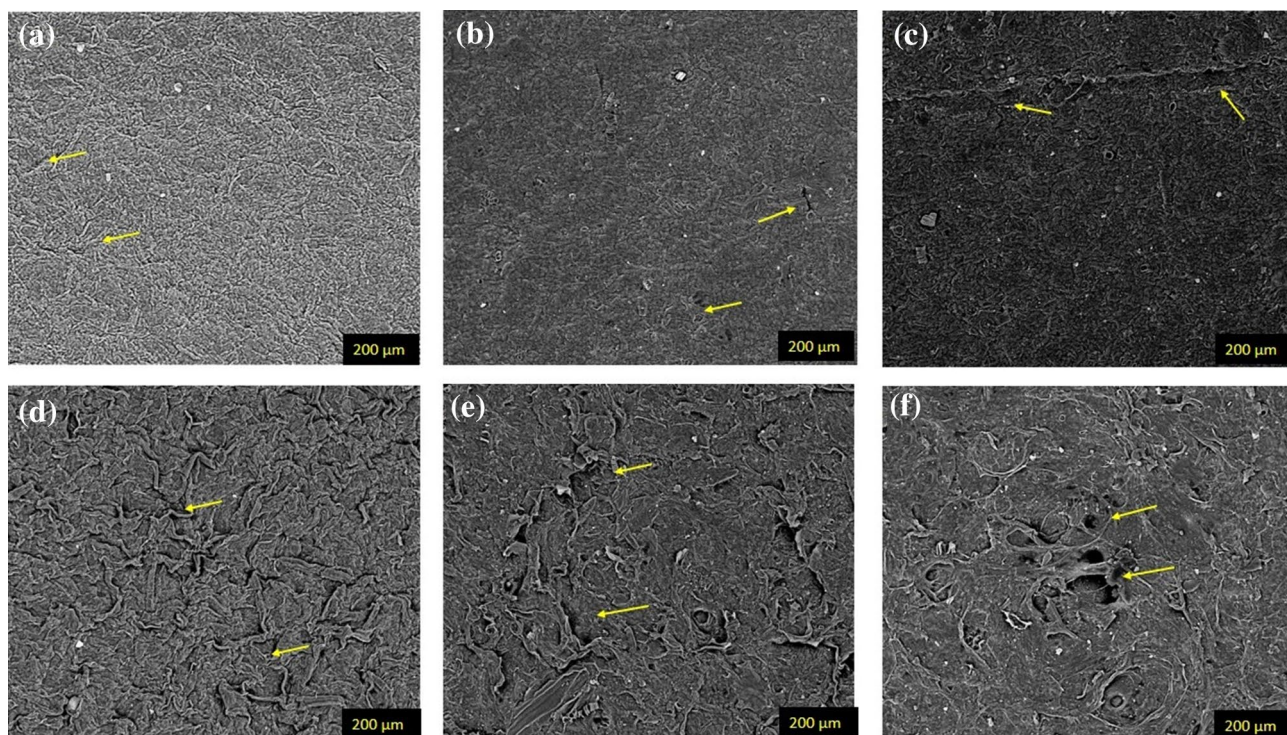


**Fig. 2** Scanning electron microscopy image at 500×magnification (200 μm scale) of eucalyptus nanocellulose (NEL), pine nanocellulose (PIN) films and blended films with different concentrations of NAC. **a** NEL control (0% NAC); **b** addition of 20% NAC with 80%

NEL; **c** addition of 35% NAC with 65% NEL; **d** PIN control (0% NAC); **e** addition of 20% NAC with 80% PIN and **f** 35% NAC with 65% PIN. Arrows indicate surface imperfections (openings)

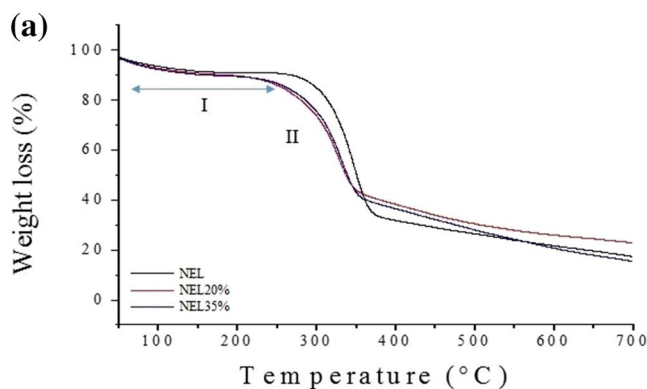
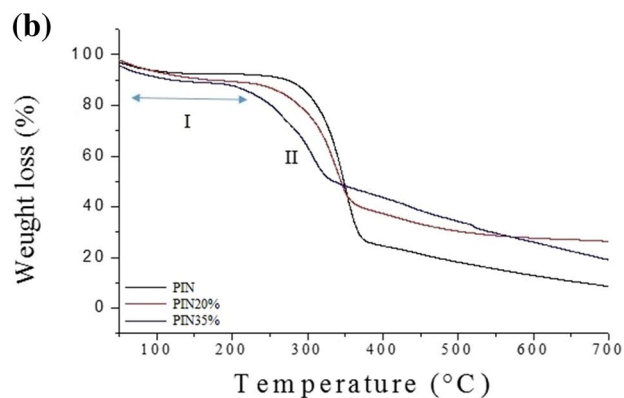


**Fig. 3** TGA of eucalyptus nanocellulose (NEL), pine nanocellulose (PIN) and blended films with different concentrations of cocoa shell nanocellulose (NAC). **a** NEL control (0% NAC), NEL20% (20%



NAC addition with 80% NEL) and NEL35% (35% NAC addition with 65% NEL); **b** PIN control (0% NAC), PIN20% (20% NAC addition with 80% PIN) and PIN35% (35% NAC addition with 65% PIN)

NAC showed similar deformation trends, and three thermal events of mass loss were identified[57].

The first thermal mass loss event occurred below 220 °C and was responsible for 7% and 9% reductions in the masses of the NEL and PIN films, respectively. According to Baruah et al. [58] moisture and other volatile materials evaporate during this thermal event. In the films containing NAC, the mass loss was greater than 10%, due to its

greater hygroscopicity. In this same temperature range, previous works reported that pineapple, sisal, kapok and banana nanocellulose also show the same mass loss behaviour, due to the breaking of intermolecular hydrogen bonds formed with chemically absorbed water molecules during melting[59, 60].

The second thermal event occurred between 220 °C and 350 °C, with the greatest reduction in film mass due to

chemical decomposition of cellulosic components during heating [48, 61]. In this thermal event, the percent mass reduction in the films containing NAC (58%) was 17% lower, when compared to the NEL and PIN films (75%) without NAC addition. It is believed that this difference in degradation can be attributed to the amounts of cellulosic and non-cellulosic components in these materials. In this sense, NEL and PIN, as they present a lower concentration of non-cellulosic components, made the film more susceptible to deterioration during heating, a result opposite to that obtained with the films containing NAC.

In the second thermal event, it was also possible to observe that the NEL films containing NAC, regardless of the concentration used, presented similar degradation curves. On the other hand, PIN films containing NAC presented distinct curves. The PIN film with the highest concentration of NAC (35%) was the first to decompose, followed by the PIN film containing 20% NAC. The difference in the decomposition temperature of these films originates from the morphology and structural dimensions of their fibres, with larger fibres, in this case those from pine, showing a high number of crystalline regions, which group together and form a heat-resistant barrier [62].

The third thermal event occurs in the temperature range above 350 °C and is responsible for the pyrolysis of cellulose, specifically the formation of carbonaceous material [63]. At this stage, the NEL and PIN control films showed the least residue formation, due to the decomposition of the crystalline region of the cellulose. Furthermore, after heating to 500 °C, the initial masses of the NEL and PIN films were partially reduced, as were those of films containing NAC, which showed greater formation of carbonaceous material related to the hemicellulose components, lignin and impurities of the NAC [62].

Furthermore, the thermal degradation of the films containing NAC presented thermogravimetric behaviour similar to that of films reported in the literature based on bleached birch nanocellulose, with three well-defined degradation events and a maximum temperature, for the third event, above 350 °C [64]. Thermal events of films produced with bleached coconut nanocellulose [59], nanocellulose from palm pulp mixed with PVA [65] and corn cob nanocellulose [66] also showed similar behaviour to the results obtained with films containing NAC.

### Contact Angle (CA)

The CA of the films were investigated, and the results are illustrated in Fig. 4. As reported by Lago et al. [13], films with CA values less than 90° are considered hydrophilic, while those with values greater than 90° are considered hydrophobic. In this case, the diffuse behaviour of the water droplet in the NEL film formed an average CA of 67.8°,

characterizing it as hydrophilic. On the other hand, PIN films, as they morphologically present fibres with anatomical characteristics superior to those of eucalyptus, presented a slightly more hydrophobic character, whose surface dispersion of the water droplet was limited, forming an angle of 70.5°. According to Oun and Rhim [50], the hydrophilicity of nanocellulose films may be a result of the large number of hydroxyl groups present in the surface layer, which is why the NEL films showed high availability of –OH and were partially more hydrophilic.

The CA of the NEL and PIN films changed with the incorporation of NAC, with 4.56% and 9.92% reductions in the respective degrees of hydrophobicity when 20% NAC was added. The differences in the surface dispersion of water droplets between these films resulted from the morphology of the film surface (smoothness/roughness), and the PIN film with 20% NAC showed less irregularity than the PIN film with the same concentration of NAC, as evidenced by SEM micrographs (Fig. 2b).

Furthermore, films with a higher concentration of NAC (35%) showed a significant reduction in the degree of hydrophobicity, greater than 33%, compared to films without NAC addition. Therefore, it can be stated that the addition of NAC above 20% considerably increased the hydrophilic character of the material, given that it allows for a greater surface interaction between water molecules and the hydroxyl groups of carboxylic acids.

In agreement with these findings, a tendency towards a reduction in CA has been reported in films made with nanocellulose isolated from cotton, where hydrophobicity decreases with increasing nanocellulose concentration [67]. In contrast, the CA of plasticized starch films reinforced with beet nanofibrils [55] and the CA of films made with nanocellulose from liquorice residues and soy protein [56] showed a structure with fewer hydroxyl groups on the surface and a consequent increase in CA. Thus, the films elaborated in this work, according to the CA results, presented hydrophilic characteristics typical of cellulosic materials and low wettability.

### Water Vapor Permeability (WVP)

The WVP (Table 2) of NEL and PIN films without addition of NAC did not differ statistically ( $p > 0.05$ ). According to Lago et al. [13], cellulosic nanofibrils have the ability to form percolated and continuous hydrogen bonding networks that reduce water vapor diffusion. Therefore, the WVP result regarding NEL and PIN is consistent, since both are clarified cellulosic materials that contain nanofibrils that tend to form a dense and compact structure during the evaporation of water molecules.

Interestingly, the WVP values observed in the films produced were lower than those of films reported in the



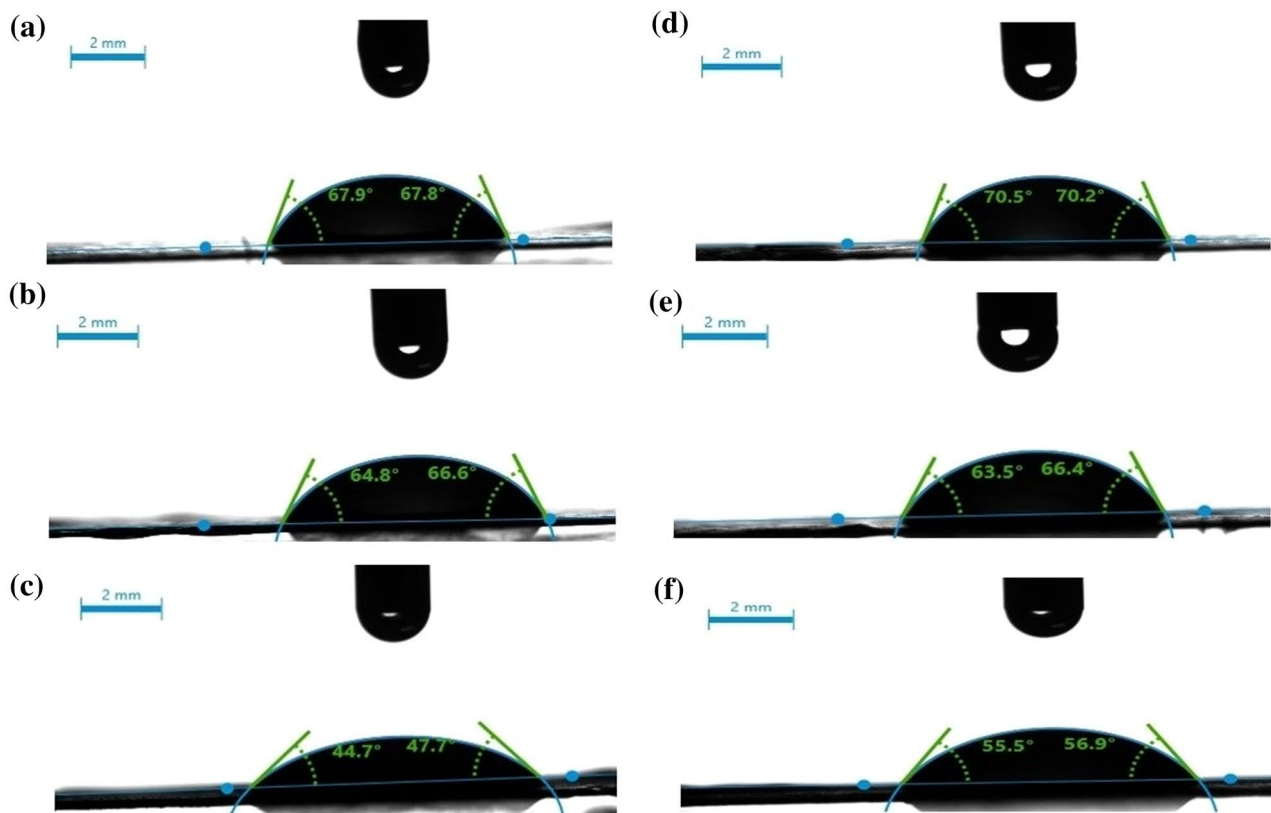


**Fig. 4** Angle of contact with water of films based on: **a** eucalyptus nanocellulose (NEL); **b** pine nanocellulose (PIN); **c** NEL20% (addition of 20% NAC with 80% NEL); **d** NEL35% (addition of 35% NAC

with 65% NEL); **e** PIN20% (addition of 20% NAC with 80% PIN) and **f** PIN35% (addition of 35% NAC with 65% PIN)

**Table 2** WVP values of films made with eucalyptus nanocellulose (NEL), pine nanocellulose (PIN) and of blended films with different concentrations of cocoa shell nanocellulose (NAC): NEL20% (addition of 20% NAC with 80% of NEL) and NEL35% (35% addition of NAC with 65% of NEL), PIN20% (20% addition of NAC with 80% of PIN) and PIN35% (35% addition of NAC with 65% of PIN)

Samples	Water vapor permeability (g mm Kpa <sup>-1</sup> dia <sup>-1</sup> m <sup>-2</sup> )
NEL	1.074 ± 0.08 <sup>a</sup>
NEL20%	1.069 ± 0.03 <sup>a</sup>
NEL35%	1.037 ± 0.04 <sup>a</sup>
PIN	1.071 ± 0.04 <sup>a</sup>
PIN20%	1.062 ± 0.05 <sup>a</sup>
PIN35%	1.052 ± 0.07 <sup>a</sup>

Lowercase letters in columns representing statistical comparisons using Tukey's test

literature and made with oat straw nanocellulose (between 1.24 and 2.53 g mm kPa<sup>-1</sup> day<sup>-1</sup> m<sup>-2</sup>) [13]. It is important to note that the difference in permeability is attributed to the way the nanofibril is structured, in addition to the specific hydrophilic characteristics of the cellulosic material [33, 68].

One of the main functions of food packaging is to prevent or minimize moisture transfer between the food and the surrounding atmosphere; therefore, WVP should be as low as possible to optimize the environment and potentially increase the shelf life of the product [13]. Thus, the films produced in this study are shown as an alternative for application in industrial processes as a barrier against atmospheric moisture in dry products or even for coating vegetables with a high respiratory rate, in which degradation essentially occurs due to waterloss [13, 69, 70].

### Solubility in Water (S)

The S values (Fig. 5) indicate that the NEL and PIN films had the lowest percent losses, about 2% and 3%, respectively. The low solubilization of the cellulose in these films is a consequence of the hydrophobic character and the strong intramolecular hydrogen bonds of the fibres present in the surface layer that limit the dispersion of water-soluble components, even when in constant agitation [71].

The incorporation of NAC in the films promoted a significant 12% increase in S (Fig. 5). This behaviour is explained by the hydrophilic components incorporated into the NAC,



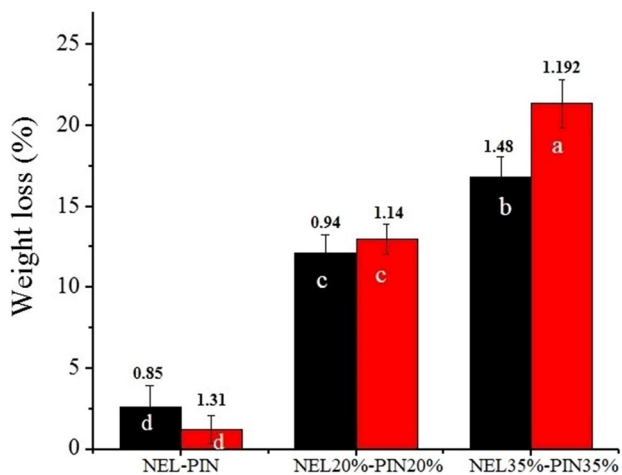


**Fig. 5** Mean and standard deviation values ( $n=3$ ) of water solubility of eucalyptus nanocellulose (NEL), pine nanocellulose (PIN) and blended films with different concentrations of cocoa shell nanocellulose (NAC): NEL20% (20% NAC addition with 80% NEL) and NEL35% (35% NAC addition with 65% NEL), PIN20% (20% NAC addition with 80% PIN) and PIN35% (addition of 35% NAC with 65% PIN). Lowercase letters on bars (a, b, c and d) representing statistical comparisons using Tukey’s test, while different letters indicate significant differences ( $p \leq 0.05$ ) between films

which formed weak hydrogen bonds between the cellulose fibres, which were easily broken during agitation in water.

Furthermore, the S values found for films containing NAC were lower than those reported in the literature for films made with cotton nanofibrils, which solubilized about 20.73% of the total mass during agitation in water [72]. Finally, the S results direct the films to be applied as

packaging or coatings for food, especially those that will be stored for a long period of time, as they guarantee protection against the external environment and, consequently, a longer shelf life of the product[73].

**Biodegradability in Soil**

The soil biodegradability of the produced films was evaluated at regular intervals by measuring weight loss in relation to time elapsed, as shown in Fig. 6. The NEL and PIN films showed the same biodegradation trends, as their total mass increased during the 168-h period (Fig. 6). This increase in mass originates from the penetration of water molecules in the polymer matrix due to the partially hygroscopic nature of the films[74], as evidenced in previous tests (CA, permeability and S).

In a 252-h period, the water that penetrated the NEL and PIN films was partially absorbed by the soil; for this reason, the residual weights of these films decreased until the 336-h mark and thereafter remained in decline until the final time of the analysis (1008 h). This low biodegradability behaviour of the NEL and PIN films may be due to changes caused by the absorption of water in the amorphous region of cellulose, inducing the formation of new structures between the nanocrystals of the micro/nanofibrils, hindering the action of deteriorating microorganisms[74].

Compared to NEL and PIN films, the addition of NAC (20% and 35%) also resulted in water absorption in the first weeks (168 h), but the absorbed water influenced the biodegradation process due to the fact that NAC contains non-cellulosic elements that increased the hydrophilic degree

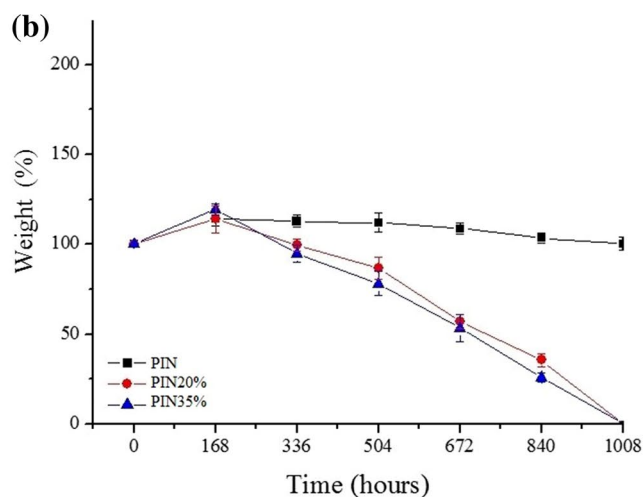
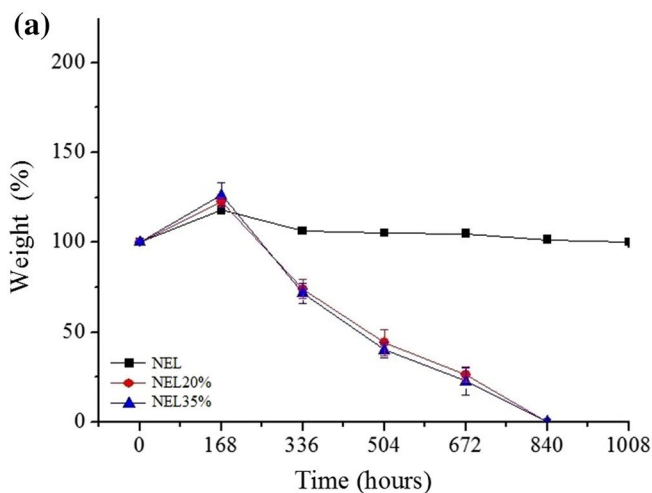


**Fig. 6** Mean and standard deviation values ( $n=3$ ) of the biodegradability of eucalyptus nanocellulose (NEL), pine nanocellulose (PIN) films and of blended films with different concentrations of cocoa shell nanocellulose (NAC). **a** NEL control (0% NAC), NEL20% (20%

NAC addition with 80% NEL) and NEL35% (35% NAC addition with 65% NEL); **b** PIN control (0% NAC), PIN20% (20% NAC addition with 80% PIN) and PIN35% (35% NAC addition with 65% PIN)

and consequently facilitated the action of deteriorating microorganisms [53].

The NEL films containing 20% and 35% NAC after the 168-h period showed rapid biodegradation with a mass loss in excess of 25% of total solids, while the PIN films containing 20% and 35% NAC were approximately 20% biodegraded. This variation in biodegradability is due to the different sizes of nanofibrils: pine has fibres with a longer length than eucalyptus fibres, in addition to a greater number of crystalline regions that can hinder the action of microorganisms [17]. In the period of 504 h, weight losses were even more significant due to the greater action of bacteria and fungi. During this period, about 50% and 35% of the weight of the total solids degraded for the NEL and PIN films containing NAC, respectively.

In the period of 672 h, weight loss greater than 75% was observed for the NEL films containing NAC, and biodegradation was complete at 840 h. The complete destruction of the NAC-added PIN films took place between 840 and 1008 h. This result was similar to that found by Babaee et al. [75] when investigating the biodegradability of films made by fibres from the kenaf stick (*Hibiscus cannabinus*) reinforced with corn starch and with glycerol/water as a plasticizer. These authors concluded that the films are fully biodegraded in the period between 40 and 60 days. Therefore, the results showed that NAC can increase the biodegradability profile of nanocellulose films considerably, making them more sustainable and ecological.

## Conclusion

This work demonstrated the use of cocoa bean shell nanofibrils (NAC) to enhance the barrier properties of films containing eucalyptus and pine nanocellulose gels. The presence of NAC did not change the water vapor permeability, but it increased the solubility of biofilms by about 12% and reduced the time to complete biodegradation of these materials. Furthermore, the TGA showed a 17% increase in the thermal stability of the films containing NAC. These results show that the technology developed can be applied and studied as a raw material for the manufacture of packaging, food coatings, reinforced polymers and drug carriers, in addition to showing itself as a sustainable solution for the management and valuation of lignocellulosic waste.

**Acknowledgements** The authors would like to thank the Coordination for the Improvement of Higher Education Personnel (CAPES), the State University of Southwest Bahia (UESB), the State University of Santa Cruz (UESC) and Bahia Research Support Foundation (FAPESB), the National Council for Scientific and Technological Development (CNPq, 405,797/2021-4).

**Data Availability** The collected data can be handed out upon request.

## Declarations

**Conflict of interest** The authors declare that they have no known competing financial interests or personal relationships that could have appeared to influence the work reported in this paper.

**Ethical Approval** This article does not contain any studies with human participants or animals performed by any of the authors.

**Informed Consent** Not applicable.

## References

- Gutiérrez, T.J., Alvarez, V.A.: Bionanocomposite films developed from corn starch and natural and modified nano-clays with or without added blueberry extract. *Food Hydrocoll.* **77**, 407–420 (2018). <https://doi.org/10.1016/j.foodhyd.2017.10.017>
- Rubentheren, V., Ward, T.A., Chee, C.Y., Nair, P., Salami, E., Fearday, C.: Effects of heat treatment on chitosan nanocomposite film reinforced with nanocrystalline cellulose and tannic acid. *Carbohydr. Polym.* **140**, 202–208 (2016). <https://doi.org/10.1016/j.carbpol.2015.12.068>
- Vanitha, R., Kavitha, C.: Development of natural cellulose fiber and its food packaging application. *Mater. Today Proc.* (2020). <https://doi.org/10.1016/j.matpr.2020.07.029>
- Taher, M.A., Zahan, K.A., Rajaie, M.A., Ring, L.C., Rashid, S.A., Mohd Nor Hamin, N.S., Nee, T.W., Yenn, T.W.: Nanocellulose as drug delivery system for honey as antimicrobial wound dressing (2020)
- Solomevich, S.O., Dmitruk, E.I., Bychkovsky, P.M., Nebytov, A.E., Yurkshovich, T.L., Golub, N.V.: Fabrication of oxidized bacterial cellulose by nitrogen dioxide in chloroform/cyclohexane as a highly loaded drug carrier for sustained release of cisplatin. *Carbohydr. Polym.* **248**, 116745 (2020). <https://doi.org/10.1016/j.carbpol.2020.116745>
- Cho, C., Kobayashi, T.: Advanced cellulose cosmetic facial masks prepared from Myanmar thanaka heartwood. *Curr. Opin. Green Sustain. Chem.* (2020). <https://doi.org/10.1016/j.cogsc.2020.100413>
- Eid, B.M., Ibrahim, N.A.: Recent developments in sustainable finishing of cellulosic textiles employing biotechnology. *J. Clean. Prod.* (2020). <https://doi.org/10.1016/j.jclepro.2020.124701>
- Ji, Y., Xu, Q., Jin, L., Fu, Y.: Cellulosic paper with high antioxidative and barrier properties obtained through incorporation of tannin into kraft pulp fibers. *Int. J. Biol. Macromol.* **162**, 678–684 (2020). <https://doi.org/10.1016/j.ijbiomac.2020.06.101>
- Nie, J., Xie, H., Zhang, M., Liang, J., Nie, S., Han, W.: Effective and facile fabrication of MOFs/cellulose composite paper for air hazards removal by virtue of in situ synthesis of MOFs/chitosan hydrogel. *Carbohydr. Polym.* **250**, 116955 (2020). <https://doi.org/10.1016/j.carbpol.2020.116955>
- Dhali, K., Ghasemlou, M., Daver, F., Cass, P., Adhikari, B.: A review of nanocellulose as a new material towards environmental sustainability. *Sci. Total Environ.* **775**, 145871 (2021). <https://doi.org/10.1016/j.scitotenv.2021.145871>
- Taheri, P., Jahanmardi, R., Koosha, M., Abdi, S.: Physical, mechanical and wound healing properties of chitosan/gelatin blend films containing tannic acid and/or bacterial nanocellulose. *Int. J. Biol. Macromol.* **154**, 421–432 (2020). <https://doi.org/10.1016/j.ijbiomac.2020.03.114>
- Phanthong, P., Reubroycharoen, P., Hao, X., Xu, G., Abudula, A., Guan, G.: Nanocellulose: extraction and application. *Carbon*

- Resour. Convers. **1**, 32–43 (2018). <https://doi.org/10.1016/j.crcon.2018.05.004>
13. Lago, R.C., do Oliveira, A.L.M., Dias, M.C., Carvalho, E.E.N., de, Tonoli, G.H.D., Boas, E.V.: Obtaining cellulosic nanofibrils from oat straw for biocomposite reinforcement: Mechanical and barrier properties. *Ind. Crops Prod.* **148**, 112264 (2020). <https://doi.org/10.1016/j.indcrop.2020.112264>
  14. Markets and Markets: Nanocellulose Market by Type (MFC & NFC, CNC/NCC, and Others), Application (Pulp&paper, composites, biomedical & pharmaceutical, electronics & sensors, and others), Region (Europe, North America, APAC, and Rest of World) - Global Forecast to 2025. (2020)
  15. Viana, L.C., De Muñiz, G.I.B., Luiz, W., Magalhães, E., De Andrade, A.S., Nisgoski, S., Potulski, D.C.: Nanostructured films produced from the bleached *Pinus sp* kraft pulp. *Floresta e Ambient.* **26**, 1–10 (2019). <https://doi.org/10.1590/2179-8087.019115>
  16. Anwar, Z., Gulfranz, M., Irshad, M.: Agro-industrial lignocellulosic biomass a key to unlock the future bio-energy: a brief review. *J. Radiat. Res. Appl. Sci.* **7**, 163–173 (2014). <https://doi.org/10.1016/j.jrras.2014.02.003>
  17. Dias, M.C., Mendonça, M.C., Damásio, R.A.P., Zidanes, U.L., Mori, F.A., Ferreira, S.R., Tonoli, G.H.D.: Influence of hemicellulose content of Eucalyptus and Pinus fibers on the grinding process for obtaining cellulose micro/nanofibrils. *Holzforschung* **73**, 1035–1046 (2019). <https://doi.org/10.1515/HF-2018-0230>
  18. Tonoli, G.H.D., Holtman, K.M., Glenn, G., Fonseca, A.S., Wood, D., Williams, T., Sa, V.A., Torres, L., Klamczynski, A., Orts, W.J.: Properties of cellulose micro/nanofibers obtained from eucalyptus pulp fiber treated with anaerobic digestate and high shear mixing. *Cellul.* (2016). <https://doi.org/10.1007/S10570-016-0890-5>
  19. Melo, E.M., Clark, J.H., Matharu, A.S.: The Hy-MASS concept: Hydrothermal microwave assisted selective scissoring of cellulose for: In situ production of (meso)porous nanocellulose fibrils and crystals. *Green Chem.* **19**, 3408–3417 (2017). <https://doi.org/10.1039/C7GC01378G>
  20. Tan, J., Li, R., Jiang, Z.T., Tang, S.H., Wang, Y.: Rapid and non-destructive prediction of methylxanthine and cocoa solid contents in dark chocolate by synchronous front-face fluorescence spectroscopy and PLSR. *J. Food Compos. Anal.* **77**, 20–27 (2019). <https://doi.org/10.1016/J.JFCA.2019.01.001>
  21. Wang, Y., Zhang, L., Liu, W., Cui, C., Hou, Q.: Fabrication of optically transparent and strong nanopaper from cellulose nanofibril based on corncob residues. *Carbohydr. Polym.* **214**, 159–166 (2019). <https://doi.org/10.1016/J.CARBPOL.2019.03.035>
  22. Eichhorn, S.J., Dufresne, A., Aranguren, M., Marcovich, N.E., Capadona, J.R., Rowan, S.J., Weder, C., Thielemans, W., Roman, M., Renneckar, S., Gindl, W., Veigel, S., Keckes, J., Yano, H., Abe, K., Nogi, M., Nakagaito, A.N., Mangalam, A., Simonsen, J., Benight, A.S., Bismarck, A., Berglund, L.A., Peijs, T.: Review: current international research into cellulose nanofibres and nanocomposites. *J. Mater. Sci.* **45**, 1–33 (2010). <https://doi.org/10.1007/S10853-009-3874-0>
  23. Soares, G.A., Alnoch, R.C., Silva Dias, G., dos Santos Reis, N., de Tavares, I.M., Ruiz, H.A., Bilal, M., de Oliveira, J.R., Krieger, N., Franco, M.: Production of a fermented solid containing lipases from *Penicillium roqueforti* ATCC 10110 and its direct employment in organic medium in ethyl oleate synthesis. *Biotechnol. Appl. Biochem.* (2021). <https://doi.org/10.1002/BAB.2202>
  24. Araujo, S.C., do Espírito Santo, E.L., de Menezes, L.H.S., de Carvalho, M.S., Tavares, I.M.C., Franco, M., de Oliveira, J.R.: Optimization of lipase production by *Penicillium roqueforti* ATCC 10110 through solid-state fermentation using agro-industrial residue based on a univariate analysis. *Prep. Biochem. Biotechnol.* (2021). <https://doi.org/10.1080/10826068.2021.1944203>
  25. de Menezes, L.H.S., Carneiro, L.L., Tavares, I.M.C., Santos, P.H., das Chagas, T.P., Mendes, A.A., da Silva, E.G.P., Franco, M., de Oliveira, J.R.: Artificial neural network hybridized with a genetic algorithm for optimization of lipase production from *Penicillium roqueforti* ATCC 10110 in solid-state fermentation. *Biocatal. Agric. Biotechnol.* **31**, 101885 (2021). <https://doi.org/10.1016/j.bcab.2020.101885>
  26. Silva, T.P., Souza, L.O., Reis, N.S., Assis, S.A., Ferreira, M.L.O., Oliveira, J.R., Oliveira, E.A., Franco, M.: Cultivation of *Penicillium roqueforti* in cocoa shell to produce and characterize its lipase extract. *Rev. Mex. Ing. Quim.* **16**(3), 745–756 (2019)
  27. Oliveira, P.C., de Brito, A.R., Pimentel, A.B., Soares, G.A., Pacheco, C.S.V., Santana, N.B., da Silva, E.G.P., Fernandes, A.G.A., Ferreira, M.M.L., Oliveira, J.R., Franco, M.: Cocoa shell for the production of endoglucanase by *Penicillium roqueforti* ATCC 10110 in solid state fermentation and biochemical properties. *Rev. Mex. Ing. Quim.* **18**(3), 777–787 (2019)
  28. Reis, N.S., Lessa, O.A., Pacheco, C.S.V., Pereira, N.E., Soares, G.A., Silva, E.G.P., Oliveira, J.R., Franco, M.: Cocoa shell as a substrate for obtaining endoglucanase and xylanase from *Aspergillus oryzae* ATCC 10124. *Acta Sci. Technol.* (2020). <https://doi.org/10.4025/actascitechnol.v42i1.48211>
  29. de Menezes, L.H.S., Ramos, M.R.M.F., Araujo, S.C., Santo, E.L.D.E., Oliveira, P.C., Tavares, I.M.C., Santos, P.H., Franco, M., de Oliveira, J.R.: Application of a constrained mixture design for lipase production by *Penicillium roqueforti* ATCC 10110 under solid-state fermentation and using agro-industrial wastes as substrate. *Prep Biochem Biotechnol* (2021). <https://doi.org/10.1080/10826068.2021.2004547>
  30. Nogueira, L.S., de Tavares, I.M., Santana, N.B., Ferrão, S.P.B., Teixeira, J.M., Costa, F.S., Silva, T.P., Pereira, H.J.V., Irfan, M., Bilal, M., de Oliveira, J.R., Franco, M.: Thermostable trypsin-like protease by *Penicillium roqueforti* secreted in cocoa shell fermentation: production optimization, characterization, and application in milk clotting. *Biotechnol. Appl. Biochem.* (2021). <https://doi.org/10.1002/BAB.2268>
  31. Reis, N.S., de Santana, N.B., Tavares, I.M.C., Lessa, O.A., dos Santos, L.R., Pereira, N.E., Soares, G.A., Oliveira, R.A., Oliveira, J.R., Franco, M.: Enzyme extraction by lab-scale hydrodistillation of ginger essential oil (*Zingiber officinale* Roscoe): chromatographic and micromorphological analyses. *Ind. Crops Prod.* **146**, 112210 (2020). <https://doi.org/10.1016/j.indcrop.2020.112210>
  32. Souza, L.O., Lessa, O.A., Dias, M.C., Tonoli, G.H.D., Rezende, D.V.B., Martins, M.A., Neves, I.C.O., de Resende, J.V., Carvalho, E.E.N., de Barros Vilas Boas, E.V., de Oliveira, J.R., Franco, M.: Study of morphological properties and rheological parameters of cellulose nanofibrils of cocoa shell (*Theobroma cacao* L.). *Carbohydr. Polym.* **214**, 152–158 (2019). <https://doi.org/10.1016/j.carbpol.2019.03.037>
  33. Hoyos, C.G., Márquez, P.M., Vélez, L.P., Guerra, A.S., Eceiza, A., Urbina, L., Velásquez-Cock, J., Rojo, P.G., Acosta, L.V., Zuluaga, R.: Cocoa shell: an industrial by-product for the preparation of suspensions of holocellulose nanofibers and fat. *Cellulose* **27**, 10873–10884 (2020). <https://doi.org/10.1007/s10570-020-03222-6>
  34. Lessa, O.A., de Carvalho Tavares, I.M., Souza, L.O., Tienne, L.G.P., Dias, M.C., Tonoli, G.H.D., de Barros Vilas Boas, E.V., Leite, S.G.F., Gutarra, M.L.E., Irfan, M., Bilal, M., Franco, M.: New biodegradable film produced from cocoa shell nanofibrils containing bioactive compounds. *J. Coatings Technol. Res.* **18**, 1613–1624 (2021). <https://doi.org/10.1007/S11998-021-00519-4>
  35. de Barros, H.E.A., Natarelli, C.V.L., Tavares, I.M.C., de Oliveira, A.L.M., Araújo, Joelma Pereira, A.B.S., Carvalho, E.E.N., Vilas Boas, E.V.B., Franco, M.: Nutritional clustering of cookies developed with cocoa shell, soy, and green banana flours using exploratory methods. *Food Bioprocess Technol.* **13**, 1566–1578 (2020). <https://doi.org/10.1007/s11947-020-02495-w>


36. Souza, F.N.S., Vieira, S.R., Campidelli, M.L.L., Rocha, R.A.R., Rodrigues, L.M.A., Santos, P.H., Carneiro, J.D.S., Tavares, I.M.C., de Oliveira, C.P.: Impact of using cocoa bean shell powder as a substitute for wheat flour on some of chocolate cake properties. *Food Chem.* **381**, 132215 (2022). <https://doi.org/10.1016/j.foodchem.2022.132215>
37. Martínez, R., Torres, P., Meneses, M.A., Figueroa, J.G., Pérez-Álvarez, J.A., Viuda-Martos, M.: Chemical, technological and in vitro antioxidant properties of cocoa (*Theobroma cacao* L.) co-products. *Food Res. Int.* **49**, 39–45 (2012). <https://doi.org/10.1016/j.foodres.2012.08.005>
38. Vásquez, Z.S., Carvalho, D.P.D., Pereira, G.V.M., Vandenberghe, L.P.S., Oliveira, P.Z.D., Tiburcio, P.B., Rogez, H.L.G., Góes, A., Soccol, C.R.: Biotechnological approaches for cocoa waste management: a review. *Waste Manag.* **90**, 72–83 (2019). <https://doi.org/10.1016/j.wasman.2019.04.030>
39. Lessa, O.A., dos Reis, N.S., Leite, S.G.F., Gutarra, M.L.E., Souza, A.O., Gualberto, S.A., Oliveirade, J.R., Aguiar-Oliveira, E., Franco, M.: Effect of the solid state fermentation of cocoa shell on the secondary metabolites, antioxidant activity, and fatty acids. *Food Sci. Biotechnol.* **27**, 107–113 (2017). <https://doi.org/10.1007/s10068-017-0196-x>
40. Lavoratti, A., Scienza, L.C., Zattera, A.J.: Dynamic-mechanical and thermomechanical properties of cellulose nanofiber/polyester resin composites. *Carbohydr. Polym.* **136**, 955–963 (2016). <https://doi.org/10.1016/j.carbpol.2015.10.008>
41. Guimarães, M., Botaro, V.R., Novack, K.M., Teixeira, F.G., Tonoli, G.H.D.: Starch/PVA-based nanocomposites reinforced with bamboo nanofibrils. *Ind. Crops Prod.* **70**, 72–83 (2015). <https://doi.org/10.1016/j.indcrop.2015.03.014>
42. Miranda, M.C., Castelo, P.A.R.: Avaliações Anatômicas das Fibras da Madeira de Parkia gigantocarpa Ducke. *Braz. J. Wood Sci.* **3**, 80–88 (2012)
43. da Silva, W.A., Pereira, J., de Carvalho, C.W.P., Ferrua, F.Q.: Determinação da cor, imagem superficial topográfica e ângulo de contato de biofilmes de diferentes fontes de amido. *Ciência e Agrotecnologia.* **31**, 154–163 (2007). <https://doi.org/10.1590/S1413-70542007000100023>
44. Bourtoom, T., Chinnan, M.S.: Preparation and properties of rice starch–chitosan blend biodegradable film. *LWT - Food Sci. Technol.* **41**, 1633–1641 (2008). <https://doi.org/10.1016/j.lwt.2007.10.014>
45. Tetens, O.: Über einige meteorologische Begriffe. (1930)
46. de Costa, É.K., Souza de, C.O., Silva, J.B.A., da Druzian, J.I.: Hydrolysis of part of cassava starch into nanocrystals leads to increased reinforcement of nanocomposite films. *J. Appl. Polym. Sci.* **134**, 1–9 (2017). <https://doi.org/10.1002/app.45311>
47. Ferrer, A., Salas, C., Rojas, O.J.: Physical, thermal, chemical and rheological characterization of cellulosic microfibrils and microparticles produced from soybean hulls. *Ind. Crops Prod.* **84**, 337–343 (2016). <https://doi.org/10.1016/j.indcrop.2016.02.014>
48. Alwani, M.S., Khalil, H.P.S.A., Islam, M.N., Sulaiman, O., Zaidon, A., Dungani, R.: Microstructural study, tensile properties, and scanning electron microscopy fractography failure analysis of various agricultural residue fibers. *J. Nat. Fibers.* **12**, 154–168 (2015). <https://doi.org/10.1080/15440478.2014.905216>
49. Vijayalakshmi, K., Neeraja, C.Y.K., Kavitha, A., Hayavadana, J.: Abaca Fibre. *Trans. Eng. Sci.* **2**, 16–19 (2014)
50. Oun, A.A., Rhim, J.W.: Effect of post-treatments and concentration of cotton linter cellulose nanocrystals on the properties of agar-based nanocomposite films. *Carbohydr. Polym.* **134**, 20–29 (2015). <https://doi.org/10.1016/j.carbpol.2015.07.053>
51. Chirayil, C.J., Joy, J., Mathew, L., Mozetic, M., Koetz, J., Thomas, S.: Isolation and characterization of cellulose nanofibrils from *Helicteres isora* plant. *Ind. Crops Prod.* **59**, 27–34 (2014). <https://doi.org/10.1016/j.indcrop.2014.04.020>
52. Moon, R.J., Martini, A., Nairn, J., Simonsen, J., Youngblood, J.: Cellulose nanomaterials review: structure, properties and nanocomposites. *Chem. Soc. Rev.* **40**, 3941–3994 (2011). <https://doi.org/10.1039/C0CS00108B>
53. Azeredo, H.M.C., Rosa, M.F., Mattoso, L.H.C.: Nanocellulose in bio-based food packaging applications. *Ind. Crops Prod.* **97**, 664–671 (2017). <https://doi.org/10.1016/j.indcrop.2016.03.013>
54. Santos, T.M., Souza Filho, M.S.M., Caceres, C.A., Rosa, M.F., Morais, J.P.S., Pinto, A.M.B., Azeredo, H.M.C.: Fish gelatin films as affected by cellulose whiskers and sonication. *Food Hydrocoll.* **41**, 113–118 (2014). <https://doi.org/10.1016/j.foodhyd.2014.04.001>
55. Li, M., Tian, X., Jin, R., Li, D.: Preparation and characterization of nanocomposite films containing starch and cellulose nanofibers. *Ind. Crops Prod.* **123**, 654–660 (2018). <https://doi.org/10.1016/j.indcrop.2018.07.043>
56. Han, Y., Yu, M., Wang, L.: Soy protein isolate nanocomposites reinforced with nanocellulose isolated from licorice residue: water sensitivity and mechanical strength. *Ind. Crops Prod.* **117**, 252–259 (2018). <https://doi.org/10.1016/j.indcrop.2018.02.028>
57. Chen, H.-B., Chiou, B.-S., Wang, Y.-Z., Schiraldi, D.A.: Biodegradable Pectin/Clay Aerogels. (2013). <https://doi.org/10.1021/am3028603>
58. Baruah, J., Deka, R.C., Kalita, E.: Greener production of microcrystalline cellulose (MCC) from *Saccharum spontaneum* (Kans grass): Statistical optimization. *Int. J. Biol. Macromol.* **154**, 672–682 (2020). <https://doi.org/10.1016/j.ijbiomac.2020.03.158>
59. Deepa, B., Abraham, E., Cordeiro, N., Mozetic, M., Mathew, A.P., Oksman, K., Faria, M., Thomas, S., Pothen, L.A.: Utilization of various lignocellulosic biomass for the production of nanocellulose: a comparative study. *Cellulose* (2015). <https://doi.org/10.1007/S10570-015-0554-X>
60. Dai, H., Ou, S., Huang, Y., Huang, H.: Utilization of pineapple peel for production of nanocellulose and film application. *Cellulose* **25**, 1743–1756 (2018). <https://doi.org/10.1007/S10570-018-1671-0>
61. Hafid, H.S., Omar, F.N., Zhu, J., Wakisaka, M.: Enhanced crystallinity and thermal properties of cellulose from rice husk using acid hydrolysis treatment. *Carbohydr. Polym.* **260**, 117789 (2021). <https://doi.org/10.1016/j.carbpol.2021.117789>
62. Li, Y., Zhu, H., Xu, M., Zhuang, Z., Xu, M., Dai, H.: High yield preparation method of thermally stable cellulose nanofibers. *BioResources* **9**, 1986–1997 (2014)
63. Oliveira, J.P. de, Bruni, G.P., Halal, S.L.M. el, Bertoldi, F.C., Dias, A.R.G., Zavareze, E. da R.: Cellulose nanocrystals from rice and oat husks and their application in aerogels for food packaging. *Int. J. Biol. Macromol.* **124**, 175–184 (2019). <https://doi.org/10.1016/j.ijbiomac.2018.11.205>
64. Asad, M., Saba, N., Asiri, A.M., Jawaid, M., Indarti, E., Wanrosli, W.D.: Preparation and characterization of nanocomposite films from oil palm pulp nanocellulose/poly (Vinyl alcohol) by casting method. *Carbohydr. Polym.* **191**, 103–111 (2018). <https://doi.org/10.1016/j.carbpol.2018.03.015>
65. Hänninen, A., Sarlin, E., Lyyra, I., Salpavaara, T., Kellomäki, M., Tuukkanen, S.: Nanocellulose and chitosan based films as low cost, green piezoelectric materials. *Carbohydr. Polym.* **202**, 418–424 (2018). <https://doi.org/10.1016/j.carbpol.2018.09.001>
66. dos Santos, R.M., Flauzino Neto, W.P., Silvério, H.A., Martins, D.F., Dantas, N.O., Pasquini, D.: Cellulose nanocrystals from pineapple leaf, a new approach for the reuse of this agro-waste. *Ind. Crops Prod.* **50**, 707–714 (2013). <https://doi.org/10.1016/j.indcrop.2013.08.049>



67. Miao, X., Lin, J., Tian, F., Li, X., Bian, F., Wang, J.: Cellulose nanofibrils extracted from the byproduct of cotton plant. *Carbohydr. Polym.* **136**, 841–850 (2016). <https://doi.org/10.1016/J.CARBPOL.2015.09.056>
68. Abdollahi, M., Alboofetileh, M., Behrooz, R., Rezaei, M., Miraki, R.: Reducing water sensitivity of alginate bio-nanocomposite film using cellulose nanoparticles. *Int. J. Biol. Macromol.* **54**, 166–173 (2013). <https://doi.org/10.1016/J.IJBIOMAC.2012.12.016>
69. Mali, S., Grossmann, M.V.E., García, M.A., Martino, M.N., Zaritzky, N.E.: Barrier, mechanical and optical properties of plasticized yam starch films. *Carbohydr. Polym.* **56**, 129–135 (2004). <https://doi.org/10.1016/J.CARBPOL.2004.01.004>
70. Assis, O.B.G., de Britto, D.: Evaluation of the antifungal properties of chitosan coating on cut apples using a non-invasive image analysis technique. *Polym. Int.* **60**, 932–936 (2011). <https://doi.org/10.1002/PI.3039>
71. Sanchez-Garcia, M.D., Gimenez, E., Lagaron, J.M.: Morphology and barrier properties of solvent cast composites of thermoplastic biopolymers and purified cellulose fibers. *Carbohydr. Polym.* **71**, 235–244 (2008). <https://doi.org/10.1016/J.CARBPOL.2007.05.041>
72. Bagde, P., Nadanathangam, V.: Mechanical, antibacterial and biodegradable properties of starch film containing bacteriocin immobilized crystalline nanocellulose. *Carbohydr. Polym.* **222**, 115021 (2019). <https://doi.org/10.1016/J.CARBPOL.2019.115021>
73. da Matta, M.D., Sarmento, S.B.S., Sarantópoulos, C.I.G.L., Zocchi, S.S.: Propriedades de barreira e solubilidade de filmes de amido de ervilha associado com goma xantana e glicerol. *Polímeros*. **21**, 67–72 (2011). <https://doi.org/10.1590/S0104-14282011005000011>
74. Matthews, J.F., Skopec, C.E., Mason, P.E., Zuccato, P., Torget, R.W., Sugiyama, J., Himmel, M.E., Brady, J.W.: Computer simulation studies of microcrystalline cellulose I $\beta$ . *Carbohydr. Res.* **341**, 138–152 (2006). <https://doi.org/10.1016/J.CARRES.2005.09.028>
75. Babaei, M., Jonoobi, M., Hamzeh, Y., Ashori, A.: Biodegradability and mechanical properties of reinforced starch nanocomposites using cellulose nanofibers. *Carbohydr. Polym.* **132**, 1–8 (2015). <https://doi.org/10.1016/J.CARBPOL.2015.06.043>

**Publisher's Note** Springer Nature remains neutral with regard to jurisdictional claims in published maps and institutional affiliations.

## Authors and Affiliations

Lucas Oliveira Souza<sup>1</sup> · Ingrid Alves Santos<sup>1</sup> · Iasnaia Maria de Carvalho Tavares<sup>1</sup> · Igor Carvalho Fontes Sampaio<sup>2</sup> · Matheus Cordazzo Dias<sup>3</sup> · Gustavo Henrique Denzin Tonoli<sup>3</sup> · Elisângela Elena Nunes de Carvalho<sup>4</sup> · Eduardo Valério de Barros Vilas Boas<sup>4</sup> · Muhammad Irfan<sup>5</sup> · Muhammad Bilal<sup>6</sup> · Julieta Rangel de Oliveira<sup>7</sup> · Marcelo Franco<sup>7</sup> 

<sup>1</sup> Department of Exact Sciences and Natural, State University of Southwest Bahia, Itapetinga 45700-000, Brazil

<sup>2</sup> Research, Innovation and Development Center, Cariacica 29140-500, Brazil

<sup>3</sup> Department of Forest Science, Federal University of Lavras, Lavras 37200-000, Brazil

<sup>4</sup> Department of Food Science, Federal University of Lavras, Lavras 37200-000, Brazil

<sup>5</sup> Department of Biotechnology, Faculty of Science, University of Sargodha, Sargodha 40100, Pakistan

<sup>6</sup> School of Life Science and Food Engineering, Huaiyin Institute of Technology, Huaian 223003, China

<sup>7</sup> Department of Exact Sciences and Technology, State University of Santa Cruz, Ilhéus 45654-370, Brazil